frontiers | Frontiers in Earth Science

TYPE Original Research
PUBLISHED 11 January 2023
DOI 10.3389/feart.2022.1092823

OPEN ACCESS

EDITED BY
Shenghong Yang,
University of Oulu, Finland

REVIEWED BY
Wei Wang,
China University of Geosciences Wuhan, China
Gaoxue Yang,
Chang'an University, China

*CORRESPONDENCE
M. P. Manu Prasanth,
manu@earth.sinica.edu.tw

SPECIALTY SECTION
This article was submitted to Petrology, a section of the journal Frontiers in Earth Science

RECEIVED 08 November 2022
ACCEPTED 28 December 2022
PUBLISHED 11 January 2023

CITATION
Manu Prasanth MP, Pang K-N, Hari KR, Sahoo BB, Ravindran A and Iizuka Y (2023), Geochemistry of Precambrian dyke swarms in the Singhbhum craton, India: Implications for recycled crustal components in the mantle source. *Front. Earth Sci.* 10:1092823. doi: 10.3389/feart.2022.1092823

Geochemistry of Precambrian dyke swarms in the Singhbhum craton, India: Implications for recycled crustal components in the mantle source

M. P. Manu Prasanth[1]*, Kwan-Nang Pang[1], K. R. Hari[2], Bibhuti Bhusan Sahoo[2,3], Arathy Ravindran[4,5] and Yoshiyuki Iizuka[1]

[1]Institute of Earth Sciences, Academia Sinica, Taipei, Taiwan, [2]School of Studies in Geology and Water Resource Management, Pt. Ravishankar Shukla University, Raipur, India, [3]Central Ground Water Board (CGWB), Northeastern region, Guwahati, India, [4]Institute of Geochemistry and Petrology, ETH Zurich, Zurich, Switzerland, [5]Institute of Geological Sciences, University of Bern, Zurich, Switzerland

The Singhbhum craton, eastern India records multiple stages of emplacement of Precambrian dyke swarms with contrasting petrogenetic models proposed for their formation. In this study, we document elemental and Sr-Nd isotopic data for three major dyke swarms in the southern part of the craton, including the ca. 2.7 Ga Ghatgaon dyke swarm, the Early Proterozoic Keonjhar dyke swarm and the ca. 1.76 Ga Pipilia dyke swarm. Dyke compositions are dominated by basalt and basaltic andesite with minor andesite, showing trace element signatures typical of continental crustal rocks. Age-corrected Nd isotopic data for Ghatgaon (ε_{Ndt} = −4.8 to + 4.6), Keonjhar (ε_{Ndt} = −11.9 to + 3.8), and Pipilia (a single sample with ε_{Ndt} = −8.8) dyke swarms display substantial variations. The lack of magma compositions that could indicate the presence of elevated mantle potential temperature among the rocks suggests melting regime was likely similar to the ambient mantle. The Dy/Yb and Dy/Dy* systematics of the rocks indicates melting occurred between spinel-stable depths and the spinel-garnet transition zone. The dominantly mafic compositions of the rocks and ubiquitous continental crustal trace element signature are best explained by peridotite source with recycled crustal components, probably in the form of pyroxenites. Our new Nd isotopic data, which argue against any simple secular evolution trend invoked in previous studies, indicate that crustal recycling was likely an episodic phenomenon rather than a discrete, single-stage process since the Archean. Geochemical modelling indicates that a sublithospheric mantle source with (10% or less) recycled crustal components satisfactorily explains the trace element variations of the dyke swarms.

KEYWORDS

precambrian, singhbhum craton (India), dyke swarms, mantle melting, crustal recycling

1 Introduction

Giant radiating dyke swarms represent conspicuous extensional structures that are widespread throughout Archean cratons and have been commonly used to reconstruct the rifting history of cratonic blocks (Wilson, 1990; Bleeker and Ernst, 2006; Söderlund et al., 2010). For example, geochronologic and paleomagnetic data for Neoarchean-Paleoproterozoic dyke swarms led to the identification and characterization of several distinct, transient, late Archean super cratons (e.g., Scalvia, Superia and Vaalbara). Although by no means universal, giant

radiating dyke swarms are considered to represent plumbing systems feeding large igneous provinces (LIPs) (Ernst, 2014; Srivastava et al., 2019; Buchan and Ernst, 2021). Dominated by basaltic compositions, the dyke swarms and their volcanic associations have been used to probe mantle source characteristics, conditions of magma genesis and processes of magma differentiation (Huppert et al., 1985; Bédard et al., 2021).

If giant radiating dyke swarms are indeed related to LIPs, then anomalously high mantle potential temperature (T_P) and hence mantle plumes might be implied. However, mantle plumes do not represent a unified explanation even for Phanerozoic LIPs. For example, the Central Atlantic Magmatic Province (CAMP) and North Atlantic Large Igneous Province (NALIP) are explained by internal heating of the upper mantle beneath thick lithosphere as a result of long-term continental insulation (Korenaga, 2004; Coltice et al., 2007; Hole, 2015; Whalen et al., 2015). The magmatism and subsequent rifting events have been ascribed to plate boundary forces associated with the breakup of Pangea (Manu Prasanth et al., 2022). Further, it has been proposed that the mantle sources of NALIP and CAMP contain significant amounts of recycled crustal materials (Korenaga, 2004; Whalen et al., 2015; Marzoli et al., 2018). Such unusually fertile sources could explain the large magma volumes associated with LIPs under ambient mantle thermal regimes (Korenaga, 2004; Coltice et al., 2007). Whether or not that applies to Precambrian dyke swarms, however, has not been explored in sufficient detail.

Precambrian dyke swarms of distinct generations are well preserved in the Singhbhum craton, India. For example, seven distinct groups of dyke swarms are identified based on emplacement ages spanning from Neoarchean to Paleoproterozoic (ca. 2.8–1.7 Ga) and are correlated with dyke swarms in other cratonic masses worldwide (Srivastava et al., 2019). However, the source and magmatic processes responsible for generating the Singhbhum dyke swarms are still controversial, with proposed origins involving a mantle plume (Srivastava et al., 2019), plume-triggered melting of subcontinental lithospheric mantle (SCLM) (Pandey et al., 2021) or interaction between enriched-depleted MORB mantle (DMM) and low degree partial melts of metasomatized SCLM (Adhikari et al., 2021). Here, we document bulk rock geochemical and Sr-Nd isotopic data to explore the mantle source characteristics and melting dynamics of the Neoarchean Ghatgaon dyke swarm (ca. 2.76–2.75 Ga), the Early Paleoproterozoic Keonjhar dyke swarm, and the Paleoproterozoic Pipilia dyke swarm (ca. 1.77 Ga) in the southern part of the Singhbhum craton (Shankar et al., 2018; Dasgupta et al., 2019; Srivastava et al., 2019; Adhikari et al., 2021; Pandey et al., 2021). Based on our new data and published data, we show that the generation of the three sets of dyke swarms most likely involved mantle sources that contain episodically recycled crustal materials.

2 Geological background

The Singhbhum craton, in eastern India, has prolonged sedimentary and magmatic records spanning the Paleoarchean to Neoproterozoic (Olierook et al., 2019). The earliest phase of major crustal growth likely occurred between 3.55 Ga and 3.32 Ga in the Paleoarchean (Upadhyay et al., 2014; Dey et al., 2017; Pandey et al., 2019), manifested in the emplacement of Paleo-Mesoarchean granitoids over two intervals at ~3.45–3.44 Ga and ~3.35–3.34 Ga, and of sodic tonalites and trondhjemites of the older metamorphic group at ~3.45–3.44 Ga. Contemporaneous evolution of older metamorphic group and parts of Iron ore group are noticed at ca. 3.5 to 3.3 Ga (Olierook et al., 2019). The craton also records earliest episode of crustal recycling during the Eoarchean. The Eoarchean detrital zircons record the crustal generation by recycling of Hadean felsic crust formed at ~4.3 to 4.2 Ga and ~3.95 Ga (Sreenivas et al., 2019). There is evidence for a drastic shift from unradiogenic to radiogenic Hf isotope compositions during Paleoarchean and Mesoarchean (~3.5 Ga to 3 Ga), which has been correlated with change in geodynamic regime of the craton (Sreenivas et al., 2019). The craton was stabilized at the end of the Paleoarchean (ca. 3.2 Ga), a period during which potassic granites formed, albeit in a sporadic manner, throughout the craton (Olierook et al., 2019; Pandey et al., 2019; Chaudhuri et al., 2022). The evolved Hf and O isotopic signatures in detrital zircons point out that reworking of existing crust was dominant at 2.67–2.35 Ga (Wang et al., 2022)

The discrete episodes of Precambrian dyke emplacement in Singhbhum craton are correlated with plumbing systems of Precambrian LIPs (Kumar et al., 2017; Srivastava et al., 2019). The Neoarchean to Paleoproterozoic (ca. 2.8–1.7 Ga) dyke swarms of the craton have been divided into seven distinct groups (Srivastava et al., 2019), and are correlated with other cratons to establish the juxtaposition of ancestral cratonic masses, that constitutes Precambrian supercontinents. The earliest dyke swarms known to have emplaced so far are ~2.8 Ga Keshargaria dyke swarm and 2.76–2.75 Ga Ghatgaon dyke swarm, which were correlated to mafic volcanic-intrusive units in the Pilbara and Kapaval Cratons (Kumar et al., 2017; Shankar et al., 2018). Kumar et al. (2017) proposed that at ~2.77 Ga, the Singhbhum, Pilbara, and Kapaval cratons were proximal to each other. Based on the paleomagnetic pole of the 1.75 Ga Pipilia swarm, Shankar et al. (2018) proposed that the Singhbhum, North China, and Baltica cratons were proximal to each other. Moreover, dyke swarms of adjacent eastern Dharwar and Bastar cratons have also been correlated with the Singhbhum dyke swarms (Pandey et al., 2021). Earlier studies named Precambrian mafic dyke swarms of the Singhbhum craton as Newer dolerites. In a recent study, based on the cross-cutting relationships, orientations, and U-Pb and Pb-Pb baddeleyite ages, Srivastava et al. (2019) classified the dyke swarms in the Singhbhum craton into seven groups: 1) NE-SW trending Keshargaria dyke swarm (ca. 2.8 Ga), 2) NNE-SSW to NE-SW-trending Ghatgaon dyke swarm (ca. 2.76–2.75 Ga), 3) NE-SW to ENE-WSW trending Kaptipada dyke swarm (2.26 Ga), 4) early Paleoproterozoic E-W to ENE-WSW Keonjhar dyke swarm, 5) Mid Proterozoic Bhagamunda dyke swarm, 6) WNW-ESE Pipilia dyke swarm (ca. 1.77 Ga), and 7) NS-NNE Barigaon dyke swarm. As indicated above, only four out of seven were radiometrically dated, and others are classified based on the cross-cutting relationship (Srivastava et al., 2019). The focus of this study is the Ghatgaon dyke swarm, the Keonjhar dyke swarm, and the Pipilia dyke swarm (Figure 1), the features of which are described in detail below.

The Ghatgaon dyke swarm is widely distributed throughout the Singhbhum craton and exhibits a general NE-SW trend (Figure 2A). Occurrences of the dykes are more extensive in the southern part of Singhbhum granites, especially north of Bagamunda and south of Pipilia. Apart from the widely distributed NE-SW trending dykes (Srivastava et al., 2019), some dykes exhibit E-W and N-S trends. Samples were collected from Badamahuladiha, Bhimkund, and Dhenkikote regions, which are in the southern part of the craton.

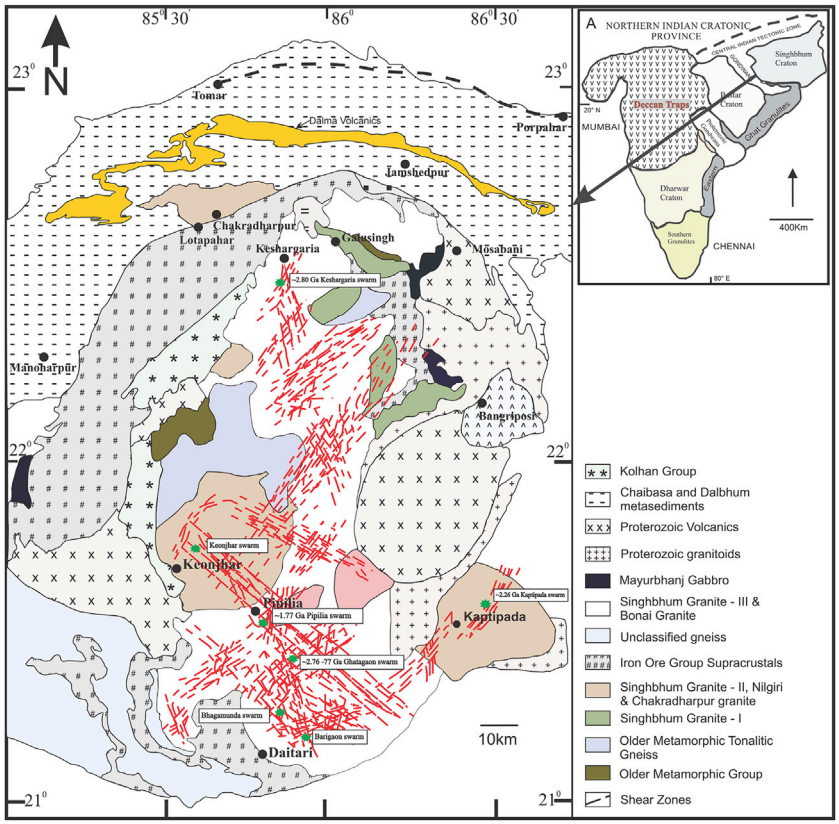

FIGURE 1
Generalized geological map of the Singhbhum craton showing the distribution of major dyke swarms (modified after Kumar et al., 2017; Srivastava et al., 2019).

The Keonjhar dyke swarm is mostly found in the southern part of the Singhbhum granite complex. Most of the Keonjhar dykes are E-W trending (Srivastava et al., 2019), although dykes exhibiting N-S and NE-SW trends could also be identified. Most of the dykes are concentrated in the Keonjhar area (Figure 2D). We collected samples from Dhurpada, Baliaguda and Ghadghadi regions. Srivastava et al. (2019) identified sporadic occurrences of Keonjhar dykes in the northern segment of Singhbhum granites and proposed an overall radiating pattern. The Pipilia dyke swarm is mostly concentrated in the Pipilia region, which is located in the southern part of Singhbhum granites. Srivasatva et al. (2019) proposed a WNW-ESE trend for the Pipilia dykes. According to our field observation, Pipilia dyke swarm exhibit N-S and NW-SE trends. Samples were collected from Pipilia and Dumuria regions. Sampling details and coordinates are given in Table 1.

3 Petrography

Most samples exhibit textures and mineralogy typical of dolerites with ubiquitous clinopyroxene and plagioclase (Figures 2B, C). Relics of olivine are observed in places among the samples. Opaque oxides (mostly Ti-magnetite and minor ilmenite) are also present sporadically. Some samples contain two populations of plagioclase, including those enclosed in the pyroxenes and also as larger zoned crystals. Petrographic observations point to the following crystallization sequence: olivine > clinopyroxene > plagioclase > Fe-Ti oxides > interstitial liquids. Most samples exhibit variable signs of alteration, the plagioclases are often replaced by clay minerals or sericite. Primary olivines, though present in small fractions, are completely replaced by iddingsite or serpentine. Pyroxenes are mostly replaced by chlorites and amphiboles.

4 Analytical methods

4.1 Major and trace element analysis

Bulk rock major and trace element analyses of fine powdered samples were carried out at CSIR-National Geophysical Research Institute, Hyderabad. The major elements were analyzed using XRF (Phillips Axios mAX4), followed by pressed pellet sample preparation technique. The details of the analytical methods, such as instrument calibration, data acquisition, accuracy, and detection limits are provided in Krishna et al. (2016). Trace elements were analyzed using AttoM HR-ICP-MS (Nu Instruments, United Kingdom). 50 mg of finely powdered samples were taken in Savillex® vials and 10 mL of the acid mixture containing HF and HNO_3 (7:3 ratio) was added. Further, the vials were heated at 150°C for 48 h and a clear solution was obtained. 1 mL of $HClO_4$ was added and the sample solutions were dried to form a solid residue. Twenty ml of 1:1 ratio HF and Millipore water mixture was added to the vials and heated at 80°C

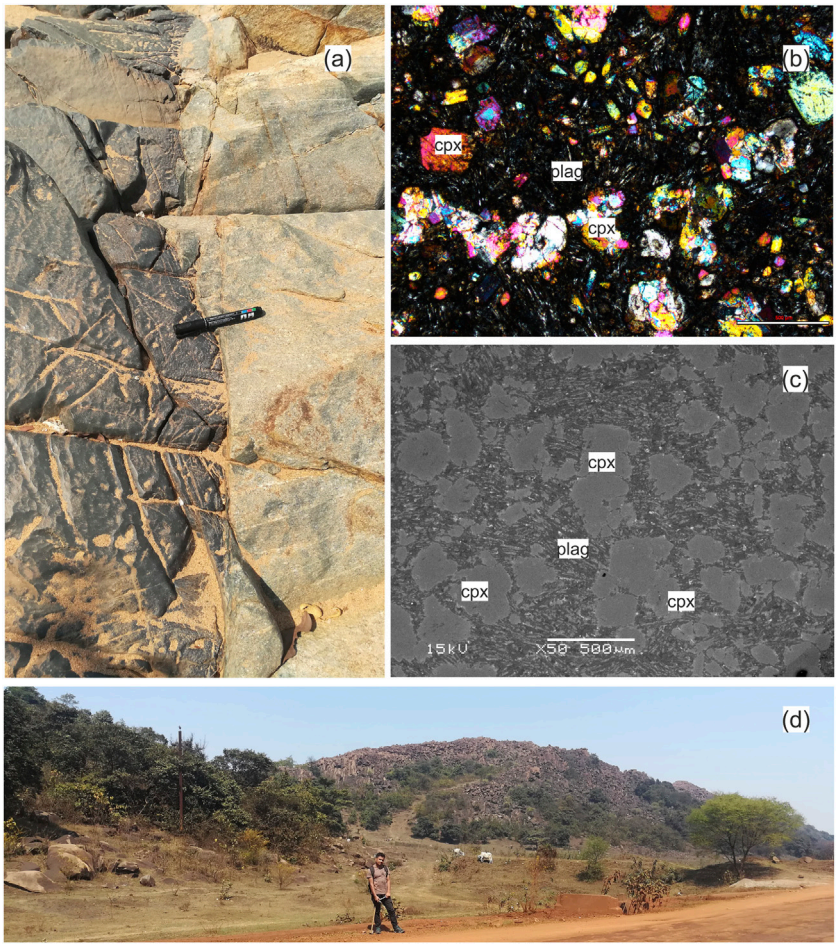

FIGURE 2
Field and petrographic images of the dyke swarms of Singhbhum craton. The field photographs of **(A)** the Ghatgaon dyke swarm shows a cross-cutting relationship with Paleoarchean TTGs and **(D)** the exposure of the Keonjhar dyke swarm in the Dhurpada area. **(B)** Petrographic and **(C)** backscattered images of the Ghatgaon dyke swarm (KD-09) show the clinopyroxene phenocrysts and the groundmass dominantly of plagioclases.

for 1 h. The sample solutions were further transferred to 25 mL conical flasks, and 5 mL of 1 ppm Rh was added as an internal standard. To obtain the optimal total dissolved solids (TDS) level, the sample solution was initially diluted to 250 mL, and 5 mL of the diluted solution is further diluted to 50 mL. The standards UB-N, JP-1 and blank solutions were analyzed along with the samples. The details of the sample digestion method, instrumental parameters, data acquisition, and quality are described in Satyanarayanan et al. (2018).

4.2 Sr-Nd isotopic analysis

Sample preparation for isotopic measurements was carried out at the Institute of Geological Sciences, University of Bern, Switzerland. Around 90 mg of finely powdered sample was spiked with ^{87}Rb-^{84}Sr and ^{149}Sm-^{150}Nd spikes in Savillex® beakers by keeping an empiric error magnification of ~1.5–2 (Stracke et al., 2014). The samples underwent a digestion procedure using concentrated HF, HNO_3 and HCl solutions separately for 2 days each at 120°C. Each step was carried out after drying the samples on a hotplate at low temperatures. After drying the samples, the samples were loaded on DOWEX® AG 50 W-X8 (200–400 mesh) cation columns to separate Rb and Sr The loading reagent was 2.5 M HCl. Rubidium and Sr cuts were collected using 2.5 M HCl with a distinct eluting step in between. Chemical separation of Sm from Nd was done using the procedure outlined by Ravindran et al. (2021).

The Rb and Sr isotopic measurements were done at the Institute of Geological Sciences, University of Bern, Switzerland. The spiked samples were measured for Rb and Sr isotopes on a Thermo Scientific™, Neptune Plus™ multi-collector inductively coupled plasma mass spectrometer (MC-ICP-MS). Dry plasma mode using a Cetac Aridus II desolvation system was used for efficient sample introduction and sensitivity during the measurements on the multi-collector ICPMS. The standards and samples were measured at the same concentration for better accuracy. Background measurements of the washing acid reagent, 0.5 M HNO_3, were subtracted from each measurement of sample and standard solutions. Interferences of ^{84}Kr and ^{86}Kr on ^{84}Sr and 86Sr were monitored and were close to the baseline ($<10^{-5}$ V). Total procedural blanks were < 500 pg that were used for the blank correction of the samples.

The Sr isotopic ratios were corrected for mass bias using exponential law and iteration (Stracke et al., 2014) with a

TABLE 1 Sample details of the dyke swarms of Singhbhum craton.

Sample no.	Area	Trend	Coordinates
Ghatgaon swarm; emplacement age = 2.76–2.75 Ga[1]			
KD-6A	Badamahuladiha	E-W	N21°36′40.1″/E085°39′00.1″
KD-6B	Badamahuladiha	E-W	N21°36′40.1″/E085°39′00.1″
KD-9	Bhimkund	N-S	N21°33′20.1″/E086°01′02.2″
KD-11	Bhimkund	N-S	N21°33′18.5″/E086°01′14.0″
KD-12A	Dhenkikote Toll	NE-SW	N21°31′48.5″/E085°48′29.6″
KD-12B	Dhenkikote Toll	NE-SW	N21°31′48.5″/E085°48′29.6″
KD-13	Dhenkikote 2	NE-SW	N21°32′51.6″/E085°47′50.9″
KD-14	Dhenkikote 2	NE-SW	N21°32′32.5″/E085°47′18.3″
Keonjhar swarm; emplacement age = early Paleoproterozoic[1]			
KD-1A	Dhurpada	E-W	N21°39′18.5″/E085°35′29.4″
KD-1B	Dhurpada	E-W	N21°39′18.5″/E085°35′29.4″
KD-2A	Dhurpada	E-W	N21°39′08.9″/E085°35′07.3″
KD-2B	Dhurpada	E-W	N21°39′08.9″/E085°35′07.3″
KD-4	Baliaguda	NE-SW	N21°39′54.8″/E085°35′17.2″
KD-5	Baliaguda	NE-SW	N21°39′51.8″/E085°35′13.2″
KD-20	Ghadghadi	N-S	N21°37′37.2″/E085°38′18.9″
KD-21	Ghadghadi	N-S	N21°37′34.1″/E085°38′17.3″
Pipilia swarm; emplacement age = 1.77 Ga[2]			
KD-7A	Dumuria	N-S	N21°34′20.1/E085°58′08.2″
KD-7B	Dumuria	N-S	N21°34′20.1″/E085°58′08.2″
KD-15A	Pipilia	NW-SE	N21°34′25.7″/ E085°46′21.06″
KD-15B	Pipilia	NW-SE	N21°34′25.7″/ E085°46′21.06″
16A	Pipilia	NW-SE	N21°34′15.7″/E085°46′28.6″
KD-16B	Pipilia	NW-SE	N21°34′15.7″/E085°46′28.6″
KD-17	Pipilia 2	N-S	N21°34′00.1″/E085°45′13.4″
KD-18	Pipilia 2	N-S	N21°33′58.1″/E085°45′22.5″
KD-19A	Pipilia 2	N-S	N21033′58.1″/E085045′22.5″
KD-19B	Pipilia 2	N-S	N21°33′58.1″/E085°45′22.5″

Age references: 1) Srivastava et al. (2019), 2) Shankar et al. (2014).

normalization ratio of $^{86}Sr/^{88}Sr$ = 0.1194. The NIST standard SRM® 987 yielded $^{87}Sr/^{86}Sr$ = 0.710253 ± 0.000012 (2SD; *n*=8). The Rb isotopic ratios were corrected for mass bias by the standard-sample-standard bracketing method using the exponential law.

Neodymium and Sm isotopes were measured on a Thermo Scientific™, Neptune™ Multi Collector ICPMS at the Institute of Geochemistry and Petrology, ETH Zurich, Switzerland. The same measurement technique used for Rb and Sr isotope measurements was carried out for Nd and Sm isotope measurements. Additionally, apart from using a normalization ratio of $^{146}Nd/^{144}Nd$ = 0.7219, Nd isotope ratios were also internally normalized for instrumental mass bias following Vance and Thirlwall (2002). Standard JNdi yielded an average $^{143}Nd/^{144}Nd$ = .512084 ± 0.000005 (2σ; *n* = 14), with an external reproducibility of 14 ppm.

4.3 Clinopyroxene composition

Analysis of clinopyroxene composition was performed at Institute of Earth Sciences, Academia Sinica, Taiwan. Selected samples were first examined with a scanning electron microscope (JEOL SEM JSM-6360LV) for microtextural observation, qualitative mineral identification, and spotting sites of interest for subsequent electron probe microanalysis (EPMA), which was undertaken by an electron probe micro analyzer (JEOL EPMA JXA-8900 R) equipped with four wavelength dispersive spectrometers (WDS). Secondary electron images and backscattered electron images were used to guide the analysis of the target positions of minerals. For quantitative analysis, a 1 μm beam was used at an acceleration voltage of 15 kV with a beam current of 12 nA. Corrections on the measured X-ray intensities were carried out by oxide-ZAF method using the standard calibration of synthetic standard minerals with various diffracting crystals. The standard minerals analyzed are as follows: wollastonite for Si with TAP crystal, rutile for Ti with PET crystal, corundum for Al (TAP), chromium oxide for Cr (PET), hematite for Fe with LiF crystal, Mn-oxide for Mn (PET), periclase for Mg (TAP), nickel oxide for Ni (LiF), wollastonite for Ca (PET), albite for Na (TAP), apatite for P (PET) and adularia for K(PET). Peak counting for each element and both upper and lower baseline X-rays counted for 10 s and 5 s, respectively. Standards run as unknowns yielded relative standard deviations of < 1% for Si, Na and K, and < 0.5% for other elements. Detection limits were less than 600 ppm for all elements. Analyses were made within the cores of mineral grains to minimize the effects of zonation, alteration and re-equilibration. The results are presented in Supplementary Table S1.

5 Results

5.1 Major and trace element geochemistry

Major and trace element data for samples from the Ghatgaon, Keonjhar and Pipilia dyke swarms are given in Supplementary Table

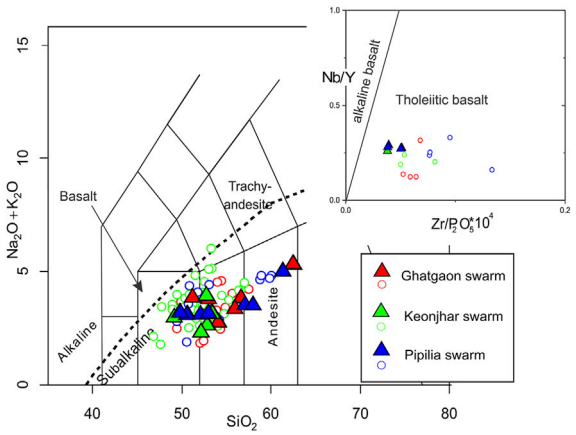

FIGURE 3
Classification of Precambrian dyke swarms of Singhbhum craton on a total alkali *versus* Silica diagram (Le Bas et al., 1986). Three major dyke swarms in the southern part of Singhbhum granite are considered for this study, including Ghatgoan (2.76 Ga), Keonjhar (Early Proterozoic) and Pipilia Swarm (1.77 Ga). Open circles indicate data from previous studies (Dasgupta et al., 2019; Adhikari et al., 2021; Pandey et al., 2021). Solid triangles indicate samples of the present study. The basalt discrimination diagram (inset) between alkaline and tholeiitic basalts is after Winchester and Floyd (1976). The samples plotted in the basalt discrimination diagram are limited to SiO_2 40 to 51 wt%. The dashed line separating alkaline and sub-alkaline compositions on the TAS plot is from Irvine and Baragar (1971).

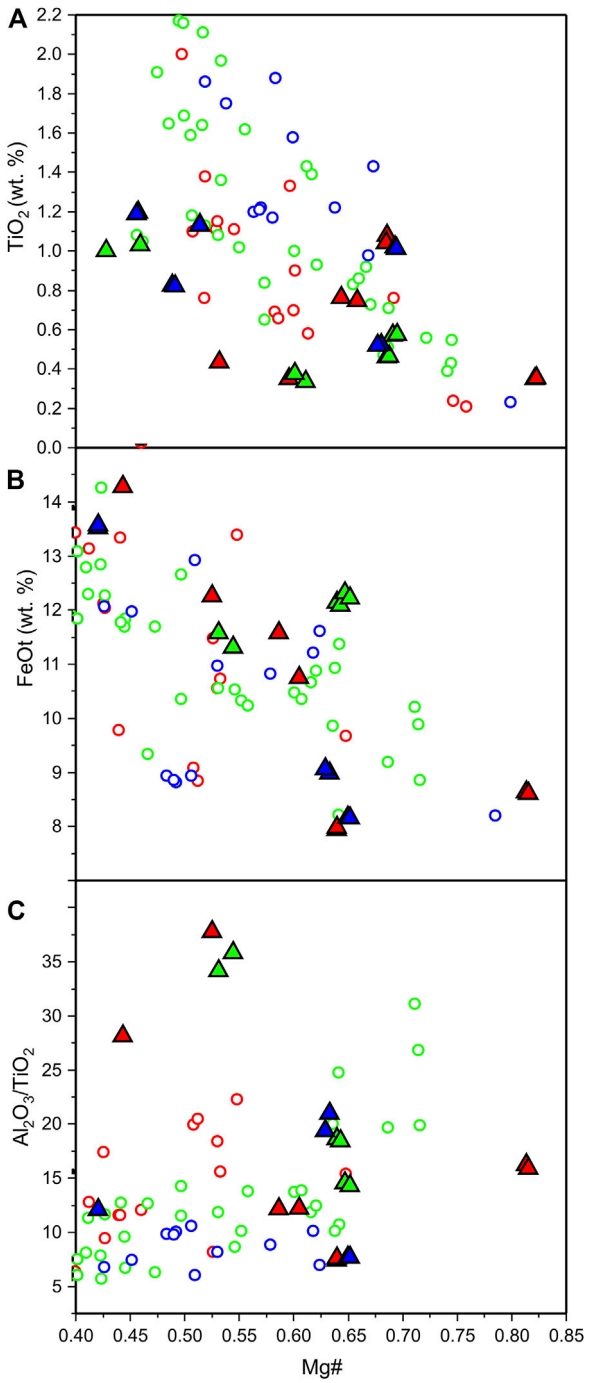

FIGURE 4
The variations of whole rock Mg-number (Mg#) against **(A)** TiO_2, **(B)** FeOt and **(C)** Al_2O_3/TiO_2. The symbols are the same as in Figure 3.

S2. Geochemical variations of the samples range from basalt, basaltic andesite to andesites (Figure 3), showing substantial compositional variations. The samples from Keonjhar exhibit compositional variations from basalt to andesites with 3.7–12.8 wt% MgO and 11.3 to 15.8 wt% FeO_t. Most of the Ghatgaon samples have 6.4 to 9.2 wt% MgO, except two samples (KD-12A, KD-12B) collected from Dhenkikote that have ~21 wt% MgO. Such high MgO is consistent with their cumulate nature. From our data and previous studies (Dasgupta et al., 2019; Adhikari et al., 2021; Pandey et al., 2021) the basalt compositions are filtered out and further plotted into Zr/P_2O_5*10^4 vs. Nb/Y diagram of Winchester and Floyd (1976) to discriminate between alkaline and tholeiitic compositions (Figure 3, inset). The dyke swarms of Ghatgaon, Keonjhar and Pipilia exhibit tholeiitic basalt compositions. A relative compositional variability is observed mainly in Ghatgaon and Pipilia dyke swarms. No systematic trend exists between TiO_2 *versus* Mg# (Figure 4). Variations in Al_2O_3/TiO_2 *versus* Mg# (Figure 4) in relatively less evolved (Mg# >50) lavas indicate moderate degree of partial melting from the mantle source (Nesbitt et al., 1979).

All samples display LREE-enriched patterns in chondrite-normalized variation diagrams (Figure 5). Though the REE patterns of Pipilia swarms are subparallel, the variations in other dyke swarms highlight the differences between the compositional variability of individual dyke swarms. Especially, sample KD-21of Keonjhar dyke swarm exhibit relatively enriched REE patterns (Figure 5C). In the multi-element diagram, compositional variations can be observed in individual dyke swarms, pointing towards a complex petrogenetic relation (Figure 5). Almost all samples exhibit negative Ti anomalies, positive Pb anomalies and negative Nb anomalies (Figure 5). The Ghatgaon samples show negative Y anomalies, whereas the Keonjhar and Pipilia samples exhibit either negative or positive Y anomalies. Negative Sr anomalies relative to Pr and Nd can also be noticed for most of the samples.

5.2 Sr-Nd isotopic compositions

The Sr-Nd isotopic data for nine selected samples with basaltic composition are listed in Table 2, which include four samples from Ghatgaon dyke swarm, four samples from Keonjhar dyke swarm and one sample from the Pipilia dyke swarm. They display large variations. For instance, initial $^{87}Sr/^{86}Sr$ of samples from Keonjhar dyke swarm ranges from .705543 to .707282, and ε_{Ndt} values from -12.0 to + 3.9 (Table 2). The lack of negative correlation between them (Figure 6) indicates the Rb-Sr isotopic system might have been disturbed by post-magmatic processes (e.g., alteration); the Sm-Nd isotopic system is relatively insensitive to such processes. Both positive and negative ε_{Nd} values are evident for the Ghatgaon and Keonjhar samples. In Keonjhar dyke swarm, the sample that exhibits relatively enriched REE patterns (KD-21) also shows an enriched ε_{Ndt} value of -12. A single sample (KD-19A) from the Pipilia dyke swarm yielded an ε_{Nd} value of -8.8.

5.3 Clinopyroxene composition

Due to the altered nature of the samples, representative samples containing fresh clinopyroxene are selected from the three dyke swarms for mineral chemical analysis. The selected samples are from the Keonjhar and Ghatgaon dyke swarms; no Pipilia samples were selected. Clinopyroxene in the Keonjhar samples exhibits mostly augitic compositions ($En_{48-36}Wo_{44-34}Fs_{22-13}$), and are characterized by 51–54 wt% of SiO_2 and 13–17 wt% MgO. Clinopyroxene in the Ghatgaon samples has compositions varying from pigeonite to augite ($En_{50-37}Wo_{36-11}Fs_{44-19}$) (Figure 7A). All analyzed clinopyroxene have relatively low TiO_2. Further, most clinopyroxene compositions plot on or below the equilibrium curve

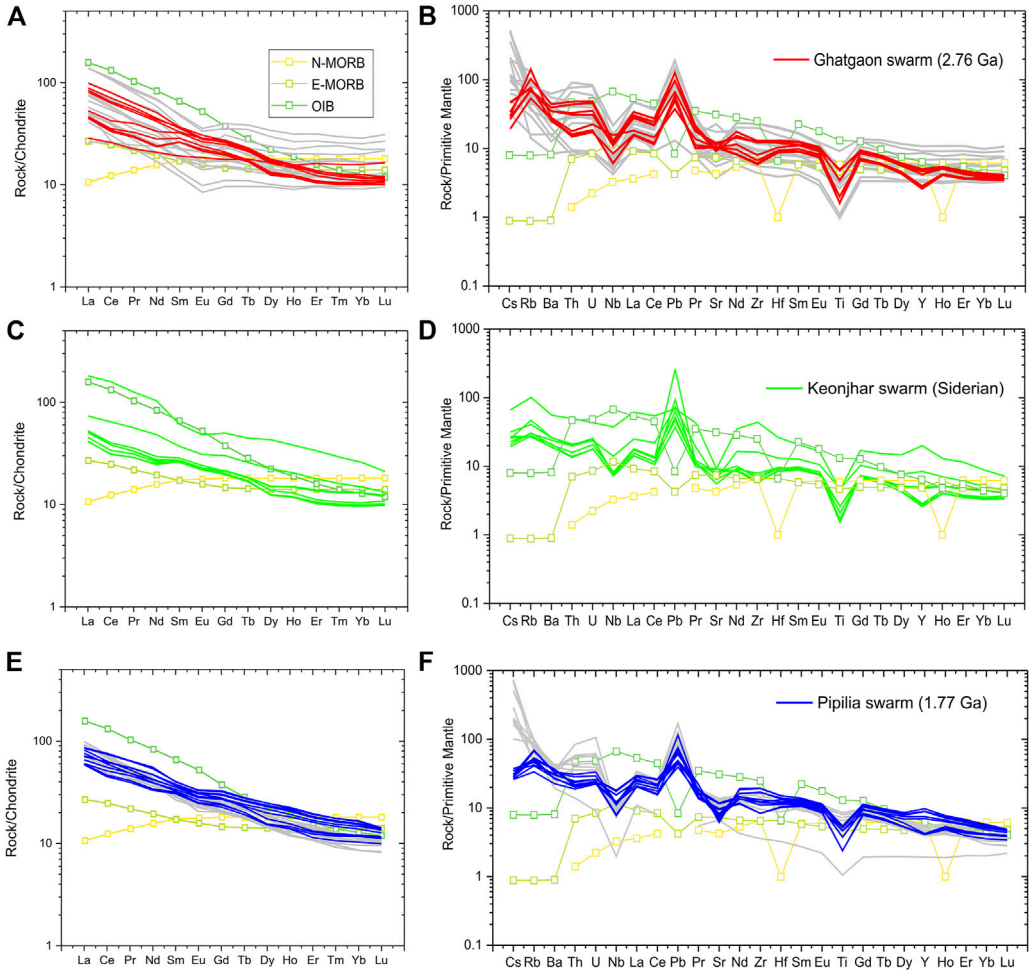

FIGURE 5
Chondrite normalized rare earth element (REE) patterns and primitive mantle normalized multi-element diagram of **(A, B)** Ghatgaon dyke swarm **(C, D)** Keonjhar dyke swarm **(E, F)** Pipilia dyke swarm. Data from the previous studies (grey lines) are also shown for comparison (Adhikari et al., 2021; Pandey et al., 2021). In the primitive mantle normalized diagram, the elements are arranged with increasing incompatibility in mantle rocks from right to left. The normalizing values of chondrite and primitive mantle are from Sun and McDonough (1989).

in the Rhodes diagram (Figure 7B), indicating most clinopyroxene grains formed by equilibrium crystallization. In other words, those grains crystallized from or continually equilibrated with the groundmass that eventually solidified as the framework of the dolerites. Compositional variations in the clinopyroxenes are also exhibit significant overlap with mid-ocean ridge basalts (MORB) and Island arc tholeiites (IAT) (Figure 7C).

6 Discussion

The samples analyzed in this study do not meet the criteria of primitive magmas in equilibrium with mantle peridotites, that is, relatively high Ni (>400–500 ppm), Cr (>1,000 ppm) and Mg# (>70) (Wilson, 1989). Instead, modest values of those geochemical parameters indicate derivation from mantle-derived magmas that underwent differentiation before solidification as the dykes. Below, we focus on three petrogenetic aspects of the dyke swarms that are indicated by available data: the origin of continental crust-like trace element signature, secular variations of Nd isotopes, characteristics of the magma source and conditions of melting.

6.1 Origin of crustal signature

The incompatible trace element patterns of the Singhbhum dykes are markedly different from typical patterns of N-MORB and OIB (Sun and McDonough, 1989). Instead, the patterns of the dykes display strong resemblance to continental crustal rocks (Figure 5). Such a trace element signature is commonly explained by assimilation of continental crustal rocks by mantle-derived magmas during their ascent to the surface, magma derivation from a mantle wedge above a subduction zone or a mantle source already modified by the crustal components. Below, we address these mechanisms in detail.

We have assessed the possibilities of crustal contamination from geochemical signatures (Figure 8A). The Nb and Th ratios have negligible effects on fractional crystallization and mantle melting, therefore the Th/Nb ratios can be used to evaluate the effect of

TABLE 2 Sr and Nd isotope data of the dyke swarms of Singhbhum craton.

Dyke swarm	Sample no	Age (Ma)	Rb (ppm)	Sr (ppm)	$^{87}Rb/^{86}Sr$	$^{87}Sr/^{86}Sr$	± 2 SE	$(^{87}Sr/^{86}Sr)i$	Sm (ppm)	Nd (ppm)	$^{147}Sm/^{144}Nd$	$^{143}Nd/^{144}Nd$	± 2 SE	$(^{143}Nd/^{144}Nd)i$	εNdt
Keonjhar	KD-1A	2400	17.488	196.916	1.1754	0.746291	0.000035	0.705543	4.037	11.465	0.13	0.511398018	0.000008	0.5093	−3.495
Keonjhar	KD-1B	2400							4.037	11.465	0.13	0.5114053	0.000004	0.5093	−3.637
Keonjhar	KD-04	2400	30.152	136.476	1.58044	0.762072	0.00006	0.707282	4.152	12.482	0.1253	0.511705408	0.000007	0.5097	3.868
Keonjhar	KD-21	2400	64.882	196.138	2.01496	0.777065	0.00003	0.707211	9.341	48.261	0.1434	0.511185092	0.000008	0.5089	−11.967
Ghatgaon	KD-6A	2762	46.717	253.881	0.47431	0.722693	0.00001	0.703721	5.036	19.486	0.1334	0.511305377	0.000007	0.5089	−3.515
Ghatgaon	KD-09 (1)	2762	91.724	221.443					4.937	15.577	0.1387	0.511815059	0.000004	0.5093	4.617
Ghatgaon	KD-09	2762	91.724	221.443	1.19683	0.755640	0.00006	0.707767	4.937	15.577	0.1388	0.511816089	0.000005	0.5093	4.577
Ghatgaon	KD-12A	2762	48.566	225.199	2.24309	0.789614	0.00017	0.699892	4.013	11.208	0.1142	0.511441158	0.000007	0.5088	−4.855
Pipilia	KD-19A	1765	26.789	129.793	0.93037	0.742145	0.00002	0.718533	6.093	25.936	0.1458	0.511594628	0.000006	0.5099	−8.856

SE= standard error of the mean; The present-day chondrite values of $^{143}Nd/^{144}Nd = 0.512638$, $^{147}Sm/^{144}Nd = 0.1967$, $^{87}Sr/^{86}Sr = 0.7045$, $^{87}Rb/^{86}Sr = 0.0827$

crustal contamination or mantle source heterogeneity (Tegner et al., 2019). The continental crust has high Th/Nb (0.875; Rudnick and Gao, 2014). The Paleoarchean and Mesoarchean TTGs and Mesoarchean K-rich granitoids of Singhbhum craton also exhibit high Th/Nb (0.786; Upadhyay et al., 2019). In the present study, samples from Ghatgaon dyke swarm (Th/Nb = 0.13–0.44), Keonjhar dyke swarm (Th/Nb= 0.15–0.32) and Pipilia dyke swarm (Th/Nb = 0.15–0.32) exhibit Th/Nb ratios lower than the continental crust, which points out that the contamination from the upper crustal sources is minimal. Further, we have evaluated the role of crustal contamination or possible involvement of recycled components in the source using the Th/Yb and Nb/Yb (Pearce, 2008). The mantle array in the Th/Yb *versus* Nb/Yb diagram represents melts formed from the oceanic mantle sources. Two mixing curves generated between MORB sources (N-MORB and E-MORB) and average continental crust (Rudnick and Gao, 2014) indicate the samples have assimilated 5% to more than 40% crustal components, in which 10%–30% of crustal contamination can explain the Th/Yb and Nb/Yb variations observed in the Pipila and Keonjhar swarms (Figure 8A). The Neoarchean Ghatgaon swarm exhibit assimilation of more than 25% of the crustal components. However, it is unlikely that a sub-alkaline primitive magma assimilates more than 20%–30% of crustal components (Heinonen et al., 2022). Roy et al. (2004) also proposed that variations in $\delta^{18}O$ (avg. + 3.97‰ ± .75‰) of newer dolerite swarms are inconsistent with the incorporation of a large volume of continental crust.

There are several differences in the geochemical and isotopic variations of the dyke swarms that cannot be easily attributed to crustal sources or assimilation of crustal components and/or magma mixing or fractional crystallization alone. The Paleoarchean granitoids of the craton are proposed to be derived from the partial melting of proto-mafic crust at ca. 10–15 kbar (Pandey et al., 2019; Upadhyay et al., 2019), formed from a near chondritic mantle reservoir (Pandey et al., 2019) (ε_{Ndt} = -0.3 to + 2.2 and ε_{Hfi} = -0.3 to + 2.0). The dyke swarms of Singhbhum craton, however, exhibit more enriched Nd isotope values. For example, part of Paleoarchean older metamorphic trondhjemite and Singhbhum granite III which are basement to the Ghatgaon dyke swarm exhibit depleted mantle values (ε_{Ndt} = + 2 .1 to + 4.5; Pandey et al., 2019). However, the Nd isotopes of the Ghatgaon samples show wide variations ($\varepsilon_{Ndt=}$+ 4.6 to -4.8). In the basement of Keonjhar swarm, the Singhbhum granite II exhibits ε_{Ndt} = + 2.7. The ε_{Ndt} values of Keonjhar dyke swarm are -11 to + 3.8. Upadhyay et al. (2019) also noticed that the Paleoarchean-Mesoarchean granites and tonalite–trondhjemite–granodiorites (TTGs) of the craton are derived from a depleted mantle source. If we recalculate the isotopic variations of basement granites it can be a potential contaminant, but it is unlikely that the observed isotopic variability results only from the assimilation of basement granitoids, as the source characteristics of the samples are inconsistent with enriched high-temperature regimes. Moreover, the mantle source characteristics appears to be similar despite their discrete emplacement ages, which points out the isotopically distinct basement granitoids cannot be attributed solely to the compositional variations.

The negative anomalies in Nb, Zr and Hf in the primitive mantle normalized diagrams (Figure 5), relatively high initial $^{87}Sr/^{86}Sr$, and negative ε_{Ndt} values can be correlated with subduction zones (Figure 6) (Zheng, 2019). Also, the clinopyroxene in the Keonjhar and Ghatgaon samples shows significant overlap between the compositional fields of clinopyroxenes from MORB and IAT (Beccaluva et al., 1989) (Figure 7C). However, similar signatures can also be produced from

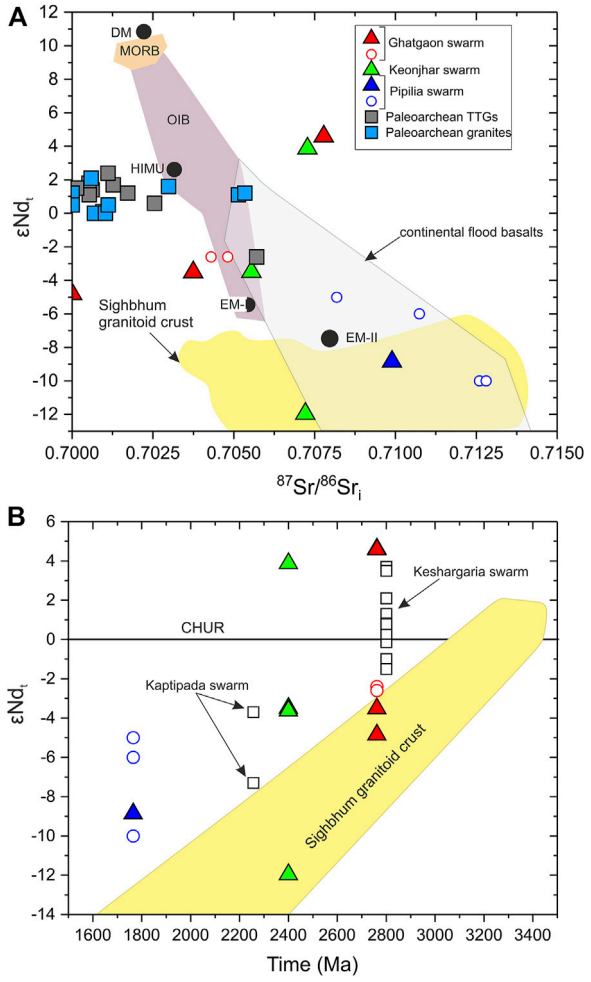

FIGURE 6
(A) Whole-rock $^{87}Sr/^{86}Sr_i$ *versus* ε_{Ndt} variations of Ghatgaon, Keonjhar and Pipilia dyke swarms. The Sr-Nd isotope variation of Paleoarchean TTGs and granites of Singhbhum craton is from Upadhyay et al. (2019). The fields and average values of the depleted mantle (DM), mid-ocean ridge basalts (MORB), ocean island basalts (OIB), OIB with high μ (HIMU), enriched mantle-1 (EM-1), enriched mantle-2 (EM-2) and continental flood basalts are from Dorais et al. (2005). Fields of Singhbhum granitoids represent recalculated values corresponding to the ages of dyke swarms. **(B)** Whole-rock ε_{Ndt} *versus* time (Ma) plot of dyke swarms of Singhbhum craton. The Nd evolution array of the Singhbhum granitoid crust from Pandey et al. (2021). Data from 2800Ma Keshargaria swarm and 2,256 Ma Kaptipada swarm (Pandey et al., 2021) are also shown for comparison.

crustal contamination or crustal components in the source. The age, distribution and cross-cutting relationship of dyke swarms are inconsistent with their origin related to a subduction zone (Figure 8) (Dasgupta et al., 2019; Adhikari et al., 2021; Pandey et al., 2021). The dyke swarms are distributed in an intracratonic regime and the stabilization of the Singhbhum craton occurred during Mesoarchean (Dey et al., 2017; Olierook et al., 2019; Srivastava et al., 2019; Hofmann et al., 2022). The emplacement of these dyke swarms occurred at discrete magmatic episodes from Neoarchean to Mesoproterozoic, and their subparallel distribution and areal extent of more than 100 km are consistent with an intracontinental rift system (Pandey et al., 2021)

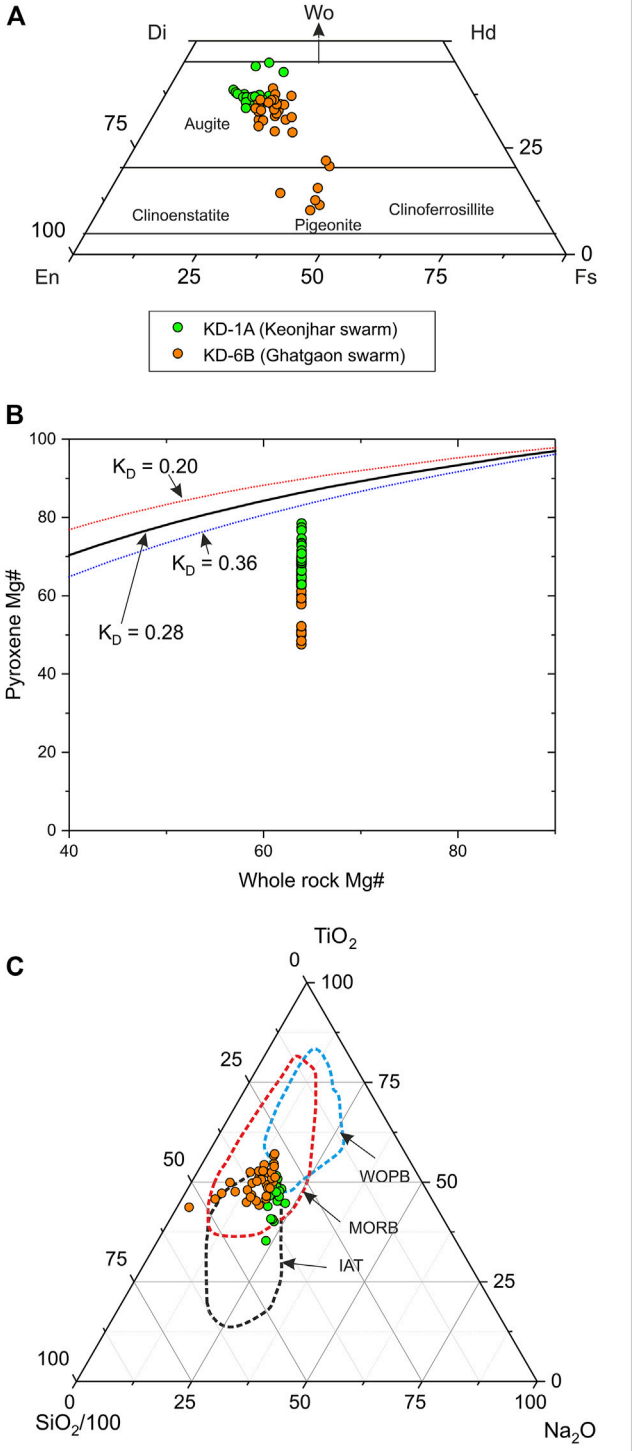

FIGURE 7
Classification of pyroxenes from Ghatgaon and Keonjhar dyke swarms. Most of the pyroxenes plot in the augite field and some from Ghatgaon exhibit distinct compositional variations. **(B)** Mineral rock Fe-Mg equilibrium diagrams for clinopyroxenes. The curves display ranges of equilibrium compositions between mineral and melt for Fe-Mg partition coefficients of .28 ± 0.08 (Putirka, 2008). **(C)** $SiO_2/100$ vs Na_2O vs TiO_2 (Beccaluva et al., 1989) discrimination diagram for clinopyroxenes from the Ghatgaon and Keonjhar dyke swarms. MORB-mid-ocean ridge basalts; IAT-island-arc tholeiites; WOPB-within ocean plate basalts.

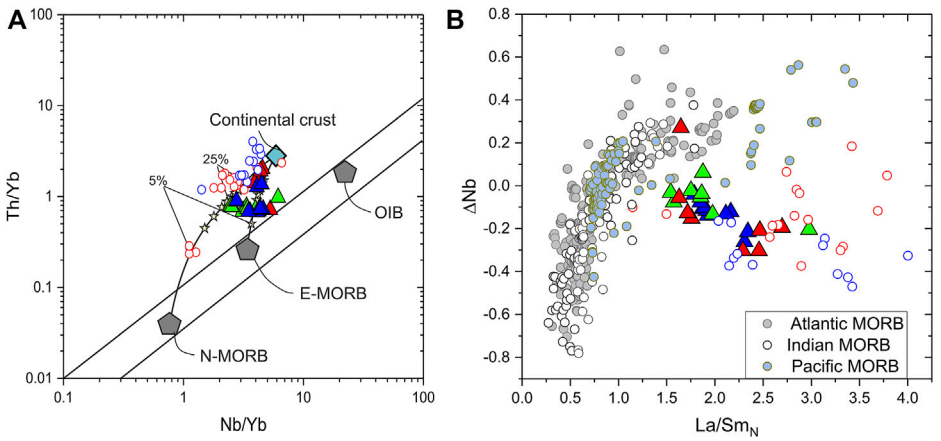

FIGURE 8
The Th/Yb *versus* Nb/Yb variations of the Ghatgaon, Keonjhar and Pipilia dyke swarm. The oceanic mantle array is from Pearce (2008). The average compositions of oceanic mantle end members include depleted mid-ocean ridge basalt or normal mid-ocean ridge basalt (N-MORB), enriched mid-ocean ridge basalt (E-MORB) and ocean island basalt (OIB) (Sun and McDonough, 1989). The average continental crust values are from Rudnick and Gao (2014). Two lines with solid yellow stars illustrate 5%–25% mixing lines of continental crust with N-MORB and E-MORB. **(B)** The ΔNb *versus* La/Sm$_N$ (normalized to primitive mantle; Sun and McDonough 1989). The Singhbhum dykes exhibit La/Sm$_N$ >1, which are consistent with LREE enriched nature (Fitton, 2007), and are compositionally distinct from midoceanic ridge basalts (MORB). The data of Atlantic, Pacific and Indian MORB are from Arevalo Jr and McDonough (2010).

We propose the observed geochemical signatures are most likely to be the characteristics of the mantle source that has incorporated crustal components (Adhikari et al., 2021; Pandey et al., 2021). Evidence for a pre-Neoarchean crustal recycling and subsequent enrichment of DMM mantle source followed by the metasomatism of SCLM has been noticed in the 2.8 Ga Jagannathpur volcanics and Ghatgaon and Keshgaria dyke swarms (Adhikari et al., 2021). Pandey et al. (2021) proposed that subduction-related crustal recycling modified the refractory SCLM. Further episodic plume impingement triggered the partial melting of the enriched SCLM between 2.8 Ga and 1.76 Ga. Moreover, delineation of thick crust under Proterozoic domains is interpreted to be evidence for Neoarchean convergent tectonics in the craton (Mandal, 2017). Recycling of Eoarchean and Paleoarchean crust (Olierook et al., 2019; Sreenivas et al., 2019; Upadhyay et al., 2019) and Mesoarchean and Neoarchean subduction-related magmatism (Mondal et al., 2006; Manikyamba et al., 2015), have been noticed in the Archean tectonic framework of Singhbhum craton. Even though the plate tectonics-related crustal recycling models during Archean are debatable (Hamilton, 2019; Zhu et al., 2021), it is conceivable that either through subduction or through non-plate tectonic modes, like melting of metasomatized lithosphere delaminated from the base of the continental crust (Cousens et al., 2001; Arndt et al., 2009), the earlier crust of Singhbhum craton have been recycled into the mantle. The resulting heterogeneous mantle source(s) can be attributed to the source of dyke swarms of Singhbhum craton (Upadhyay et al., 2014; Olierook et al., 2019; Pandey et al., 2019; Hofmann et al., 2022).

6.2 Source characteristics and melting conditions

Earlier discussion arrived at a view that the mantle source giving rise to the studied Singhbhum dyke swarms acquired a crustal trace element signature. Logical questions that follow are in which part of the mantle did that source reside, and how did it partially melted to yield the magmas that eventually solidified as the dykes. This section addresses issues relevant to geochemical and mineralogical characteristics of the mantle source, and temperature-pressure of partial melting.

First, we employ the parameter ΔNb to examine the relative enrichment and depletion of the mantle source. Calculated as 1.74+ log(Nb/Y) - 1.92 log(Zr/Y), ΔNb is used to express deviation from a reference line (i.e., ΔNb = 0) separating enriched oceanic mantle end-members (E-MORB and OIB) and N-MORB (Fitton, 2007). Fitton (2007) proposed that all N-MORB has ΔNb<0, whereas E-MORB and OIB lavas exhibit ΔNb>0. Figure 8B shows the ΔNb variations of the Gatagaon, Keonjhar and Pipilia dyke swarms. The Ghatgaon and Keonjhar dyke swarms exhibit both positive and negative ΔNb values, whereas the Pipilia dyke swarm exhibit mostly negative ΔNb values. One sample from Ghatgaon (KD-09) exhibits a maximum ΔNb of + 0.27, which means Nb is enriched 2.7 times relative to the ΔNb of zero. Other positive ΔNb values of Ghatgaon dyke swarm range from + 0.04 to + 0.18. One sample from the Keonjhar dyke swarm (KD-05) exhibits + 0.06 ΔNb whereas others exhibit negative ΔNb (-0.2 to -0.5). The variations in the ΔNb values also indicate a heterogeneous mantle source, that has both enriched and depleted components and which is distinct from MORB sources (Figure 8B). Along with ΔNb, elevated La/Sm$_n$ values illustrate high degrees of partial melting or a less depleted source (Figure 8B). Most of the ΔNb values overlap in all three dyke swarms, which again illustrates secular compositional variations (e.g., Pandey et al., 2021) in the mantle source may not be applicable, rather it can be attributed to mantle heterogeneity.

Further, we used the variations in MREE to HREE to evaluate the effects of residual garnet in the source, as garnet prefers HREE relative to MREE. The (Dy/Yb)$_N$ ratios (Davidson et al., 2013), along with (La/Sm)$_N$ ratios have been considered as they reflect the degree of mantle melting (Figure 9) (Tegner et al., 2019). The Keonjhar swarm and Ghatgaon swarms exhibit Dy/Yb of 1.8 and 1.9 (median)

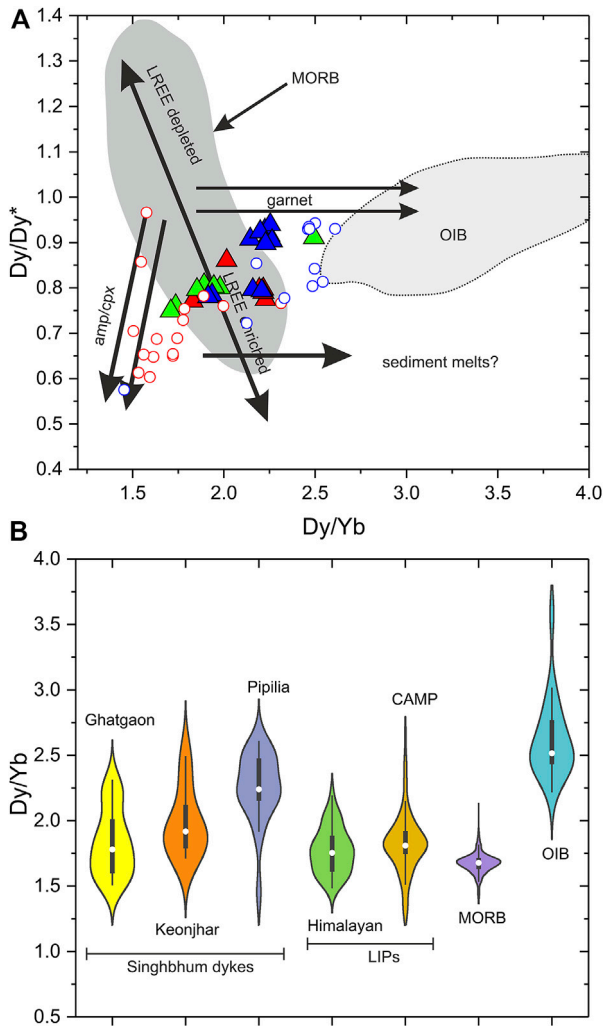

FIGURE 9
(A) Dy/Yb *versus* Dy/Dy* variation (Davidson et al., 2013) of Ghatgaon, Pipilia and Keonjhar dyke swarms. The REE values in the Dy/Dy* calculation are normalized to the values reported in McDonough and Sun (1995). **(B)** Violin plot with box plots inside illustrating the variation of Dy/Yb ratios of Ghatgaon, Keonjhar and Pipilia dyke swarms. Large igneous provinces are sourced from a subduction-modified mantle, which includes the Himalayan magmatic province and CAMP (Data source: Manu Prasanth et al., 2022). The ocean island basalt (OIB) data from Hawaii (from The GEOROC Database: https://georoc.eu/georoc/new-start.asp), and Global MORB variations, which include N-MORB and E-MORB data (Arevalo Jr and McDonough, 2010) are also shown for comparison. White circles inside the box represent mean values.

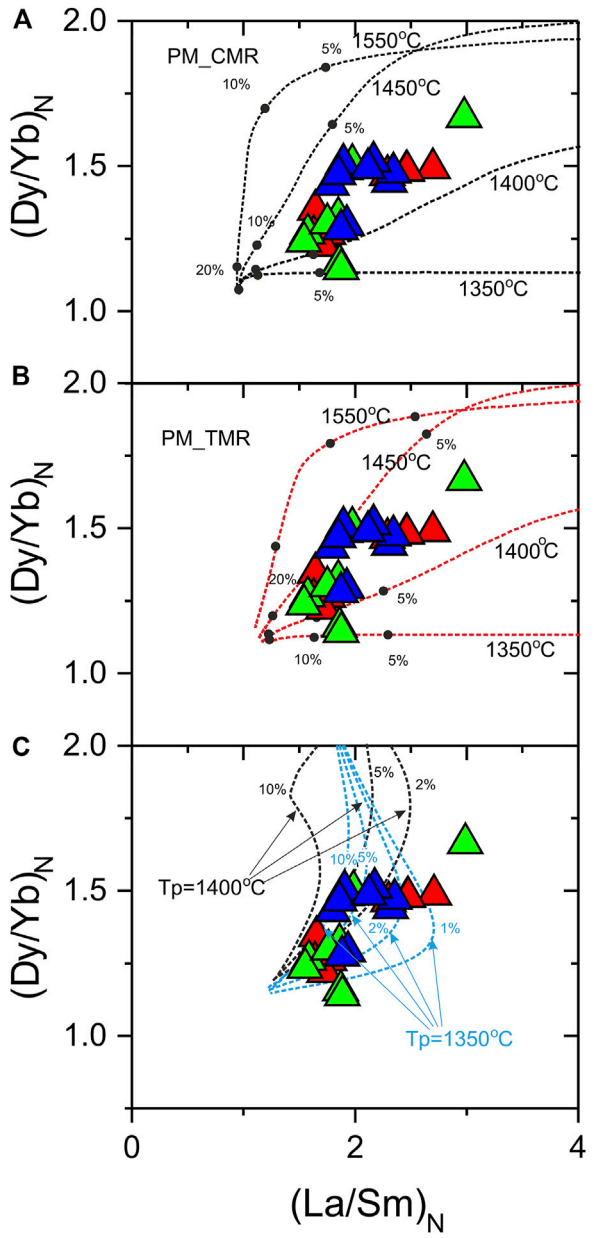

FIGURE 10
$(La/Sm)_N$ *versus* $(Dy/Yb)_N$ of the Ghatagaon, Keonjhar and Pipilia dyke swarms. **(A)** Forward models produced by melting primitive mantle in a columnar melting regime (PM_CMR) (McDonough and Sun, 1995) at mantle potential temperature from 1350°C to 1550°C. **(B)** Forward melting models produced by melting primitive mantle in a triangular melting regime (PM_CMR) (McDonough and Sun, 1995) at the same mantle potential temperatures in **(A)**. Black circles in the melting trajectories represent the degree of melting. **(C)** Forward model melts produced by melting hybrid lithologies of peridotite and pyroxenite (McDonough and Sun, 1995; Pertermann and Hirschmann, 2003). The mantle potential temperature is constrained between 1350°C and 1400°C and the proportions of pyroxenites in the source are indicated in percentage.

whereas the Pipilia swarm exhibit Dy/Yb =2.2. The Dy/Yb variations are slightly higher than MORB values (~1.6) and considerably lower than the OIB values (~2.5) (Figure 9B). The Himalayan magmatic province and CAMP proposed to be derived from a subduction-modified mantle source (Tegner et al., 2019; Manu Prasanth et al., 2022) also show overlap with the Dy/Yb variations of the Ghatgaon, Keonjhar and Pipilia swarms (Figure 10). The Dy/Dy* vs. Dy/Yb (Davidson et al., 2013), relations exhibit LREE enriched field with garnet control on some of the Keonjhar and Pipilia swarms. Most of the Ghatgaon swarm samples exhibit clinopyroxene fractionation (Figure 9A). Some samples from Dhenkikote area of Ghatgaon dyke swarm (KD-12A, KD-12B) possibly stalled at the base of the crust or coalesced into magma chambers as it is evident form their cumulate nature.

The primary magma calculation schemes depend on the addition or removal of olivine (e.g., Herzberg and Asimov, 2015; Lee et al.,

2009) were not able to retrieve realistic thermal and melting conditions as the dyke swarms exhibit fractionation of clinopyroxenes (Figure 4). Therefore, we further explored the mantle melting models using the REEBOX PRO application of Brown and Leshar (2016). This application model the composition of melts produced by lithologically heterogeneous dynamically upwelling mantle. We simulated a range of forward partial melting models of peridotitic and mixed peridotite and pyroxenite source lithologies, using different modes of melting, and variable mantle potential temperatures. The pyroxenites in the model represent recycled crustal domains in the mantle (Figure 9).

For the first two models (Figures 10A, B), we used a pyrolite peridotite source (Sun and McDonough, 1989). In the first model (Figure 10A), we used the columnar melting regime and T_p is constrained between 1350°C to 1550°C, which shows trace element variations can be achieved by 5%–10% partial melting under a T_p of 1400°C to 1,450°C. Two samples from the Keonjhar dyke swarm exhibit melting within the T_p range of 1350°C–1400°C. At 10% of melting (T_p = 1450°C–1350°C) the pressure is 2.4 to 1.3 GPa which indicates melting in the garnet-spinel transition zone and spinel peridotite zone (Su et al., 2010), and also corroborate Dy/Yb variations and both positive and negative anomalies of Y in the primitive mantle normalized diagrams (Figure 5).

In the second model (Figure 10B), we simulated a triangular melting regime with a pyrolite source as the starting composition. Relatively lower T_p (1350°C–1400°C) and 5%–10% of melting can produce compositional variations in some of the Keonjhar dyke swarms. When the T_p increases (1400°C–1450°C), 10%–20% melting is required to produce the compositional variation. Most of the melting took place in the spinel stability field. (Brown and Lesher, 2016).

To address the heterogeneous nature of the mantle source we used combinations of peridotite and pyroxenite under a columnar melting region in the third model. Considering the thick continental lithosphere of the Singhbhum craton and discrete episodes of dyke emplacement, we assumed the columnar melting region is more appropriate (Brown and Lesher, 2016; Tegner et al., 2019). Along with pyrolite peridotite, we also tried modelling with a depleted mantle (Workman and Hart, 2005) with different proportions of pyroxenites. But the melting curves did not follow the observed compositional variations. The results show anhydrous pyrolite peridotite (T_p = 1,350°C and 1,400°C) with 1%–10% pyroxenite (silica-saturated pyroxenite, G2; Pertermann and Hirschmann, 2003) were involved in the petrogenesis.

The SCLM sources combined with convecting asthenospheric regions likely contributed to the wide range of compositions in the dyke swarms of Singhbhum craton (Kamenetsky et al., 2017). The geochemical variations can be compared with LIPs like the Himalayan magmatic province, Central Atlantic Magmatic Province and North Atlantic Magmatic Province (Korenaga, 2004; Coltice et al., 2007; Marzoli et al., 2018; Tegner et al., 2019; Manu Prasanth et al., 2022), as their origins are inconsistent with a deep-seated mantle plume and are proposed to be derived from lithospheric and/or asthenospheric mantle sources with recycled crustal components (Korenaga, 2004; Shellnutt et al., 2021; Manu Prasanth et al., 2022). Narrow zone upwelling of asthenospheric melts associated with the discrete rifting events in the craton might have triggered the melting of the lithospheric mantle domains (Foley, 2008; Tang et al., 2013), which led to the melt generation and emplacement of Ghatgaon, Keonjhar and Pipilia dyke swarms.

6.3 On secular Nd isotopic trends

Pandey et al. (2021) identified a secular Nd isotopic evolution trend for the dyke swarms of Singhbhum craton. In detail, the 2.8 Ga Keshgaria swarm exhibit near chondritic ε_{Ndt} values (-1.0 to + 2.1), whereas younger generations of dyke swarms have progressively more negative values. Such a trend is consistent with a lithospheric mantle source in which crustal materials were incubated since ~2.8–3.0 Ga, and the dyke swarms formed by periodic melt extraction from that source. However, our new data hint complexity beyond a simple, secular Nd isotopic trend. The 2.76 Ga Ghatgaon dyke swarm, which yielded negative ε_{Ndt} (-2.4 to -2.6) values (Pandey et al., 2021), displays a greater range of ε_{Ndt} values from negative to positive (ε_{Ndt} = -4.8 to + 4.6). Also, the Neoarchean-Paleoproterozoic Keonjhar dyke swarm exhibits a similar but more extreme range of ε_{Ndt} values (ε_{Ndt} = -11.9 to + 3.8) (Figure 6). Undoubtedly, at least for the Ghatgaon and Keonjhar dyke swarms, a depleted mantle-like component must also be involved at the time of magma genesis. One way to explain the Nd isotopic range was interaction between asthenosphere and mantle lithosphere that had been previously enriched. However, samples having positive ε_{Ndt} values in this study also show continental crust-like trace element signature as strong as samples having negative ε_{Ndt} values, inconsistent with variable degrees of asthenosphere-lithosphere interaction. An alternative explanation is that the positive ε_{Ndt} values reflect recent mantle enrichment relative to the formation age of the Ghatgaon and Keonjhar dyke swarms. If the secular trend argued by Pandey et al. (2021) tracks evolution of an enriched mantle source formed by recycling of ~2.8–3.0 Ga crustal material, our new data imply that crustal materials younger than that range might also be involved, implying crustal recycling might have been episodic rather than a discrete, single-stage process. In other words, there might be multiple secular trends depending on the age of the recycled material(s). We suggest that this mechanism offers a better explanation for all Nd isotopic data available for the Singhbhum dyke swarms so far.

7 Conclusion

1) The samples from Ghatgaon, Keonjhar and Pipilia dyke swarms are best explained by a mantle source that has recycled crustal components.
2) The petrogenetic modelling indicates dominantly peridotitic source have incorporated pyroxenites through crustal recycling. Partial melting of this hybrid mantle source within the spinel stability field and spinel-garnet transition zones can explain the trace element variability of Ghatgaon, Keonjhar and Pipilia dyke swarms.
3) Thermal regimes inferred from the trace element modelling show that dyke swarms are inconsistent with a mantle plume-related origin and can be comparable with non-plume-related LIPs.
4) Crustal recycling in Singhbhum craton might have been episodic rather than a discrete, single-stage process as proposed by previous studies.

Data availability statement

The original contributions presented in the study are included in the article/Supplementary Material, further inquiries can be directed to the corresponding author.

Author contributions

MM developed the idea, interpreted the data, wrote the manuscript, and created figures. BS, YI and AR contributed to the sample preparation and analysis. K-NP and KRH contributed to the interpretations and manuscript preparation.

Funding

Financial support from the National Science and Technology Council, Taiwan (111-2116-M-001-031 to K-NP) is acknowledged.

Acknowledgments

We are grateful to Amulya Sahoo for their assistance with fieldwork. BS acknowledges a fellowship from CSIR (India) from 2016 to 2018. MM acknowledge the postdoctoral fellowship from the National Science and Technology Council, Taiwan. AR is grateful to Martin Wille and Sukalpa Chatterjee at the University of Bern for their help during isotope measurements. AR is also thankful to Bradley Peters and Jörg Rickli for the JNdi standard and useful comments on the measurement protocol of Sm and Nd isotopes.

Conflict of interest

The authors declare that the research was conducted in the absence of any commercial or financial relationships that could be construed as a potential conflict of interest.

Publisher's note

All claims expressed in this article are solely those of the authors and do not necessarily represent those of their affiliated organizations, or those of the publisher, the editors and the reviewers. Any product that may be evaluated in this article, or claim that may be made by its manufacturer, is not guaranteed or endorsed by the publisher.

Supplementary material

The Supplementary Material for this article can be found online at: https://www.frontiersin.org/articles/10.3389/feart.2022.1092823/full#supplementary-material

References

Adhikari, A., Nandi, A., Mukherjee, S., and Vadlamani, R. (2021). Petrogenesis of Neoarchean (2.80–2.75 Ga) Jagannathpur volcanics and the Ghatgaon and Keshargaria dyke swarms, Singhbhum craton, eastern India: Geochemical, SrNd isotopic and SmNd geochronologic constraints for interaction of enriched-DMM derived magma with metasomatised subcontinental lithospheric mantle. *Lithos* 400, 106373. doi:10.1016/j.lithos.2021.106373

Arevalo, R., Jr, and McDonough, W. F. (2010). Chemical variations and regional diversity observed in MORB. *Chem. Geol* 271, 70–85. doi:10.1016/j.chemgeo.2009.12.013

Beccaluva, L., Macciotta, G., Piccardo, G. B., and Zeda, O. (1989). Clinopyroxene composition of ophiolite basalts as petrogenetic indicator. *Chem. Geol* 77, 165–182. doi:10.1016/0009-2541(89)90073-9

Bédard, J. H., Troll, V. R., Deegan, F. M., Tegner, C., Saumur, B. M., and Evenchick, C. A., (2021). High arctic large igneous province alkaline rocks in Canada: Evidence for multiple mantle components. *J. Petrology* 62, egab042. doi:10.1093/petrology/egab042

Bleeker, W., and Ernst, R. (2006). Short-lived mantle generated magmatic events and their dyke swarms: The key unlocking earth's paleogeographic record back to 2.6 Ga. *Dyke swarms—time markers crustal Evol*, 3–26.

Brown, E. L., and Lesher, C. E. (2016). Reebox PRO: A forward model simulating melting of thermally and lithologically variable upwelling mantle. *Geochem. Geophys. Geosystems* 17, 3929–3968. doi:10.1002/2016gc006579

Buchan, K. L., and Ernst, R. E. (2021). Plumbing systems of large igneous provinces (LIPs) on Earth and Venus: Investigating the role of giant circumferential and radiating dyke swarms, coronae and novae, and mid-crustal intrusive complexes. *Gondwana Res* 100, 25–43. doi:10.1016/j.gr.2021.02.014

Chaudhuri, T., Kamei, A., Das, M., Mazumder, R., and Owada, M. (2022). Evolution of the archean felsic crust of singhbhum craton, india: A reassessment. *Earth-Science Reviews*. 231, doi:10.1016/j.earscirev.2022.104067

Coltice, N., Phillips, B. R., Bertrand, H., Ricard, Y., and Rey, P. (2007). Global warming of the mantle at the origin of flood basalts over supercontinents. *Geology* 35, 391–394. doi:10.1130/g23240a.1

Dasgupta, P., Ray, A., and Chakraborti, T. M. (2019). Geochemical characterisation of the Neoarchaean newer dolerite dykes of the Bahalda region, Singhbhum craton, Odisha, India: Implication for petrogenesis. *J. Earth Syst. Sci* 128, 216–223. doi:10.1007/s12040-019-1228-0

Davidson, J., Turner, S., and Plank, T. (2013). Dy/Dy*: Variations arising from mantle sources and petrogenetic processes. *J. Petrology* 54, 525–537. doi:10.1093/petrology/egs076

Dey, S., Topno, A., Liu, Y., and Zong, K. (2017). Generation and evolution of Palaeoarchaean continental crust in the central part of the Singhbhum craton, eastern India. *Precambrian Res* 298, 268–291. doi:10.1016/j.precamres.2017.06.009

Dorais, M. J., Harper, M., Larson, S., Nugroho, H., Richardson, P., and Roosmawati, N. (2005). A comparison of eastern north America and coastal new england magma suites: Implications for subcontinental mantle evolution and the broad-terrane hypothesis. *Can. J. Earth Sci* 42, 1571–1587. doi:10.1139/e05-056

Ernst, R. E. (2014). *Large Igneous Provinces*. Cambridge University Press. Cambridge, UK

Fitton, J. G. (2007). The OIB paradox, 430. *Special Papers-Geological Society Of America*, 387.

Foley, S. F. (2008). Rejuvenation and erosion of the cratonic lithosphere. *Nat. Geosci* 1, 503–510. doi:10.1038/ngeo261

Hamilton, W. B. (2019). Toward a myth-free geodynamic history of Earth and its neighbors. *Earth-Science Rev* 198, 102905. doi:10.1016/j.earscirev.2019.102905

Heinonen, J. S., Spera, F. J., and Bohrson, W. A. (2022). Thermodynamic limits for assimilation of silicate crust in primitive magmas. *Geology* 50, 81–85. doi:10.1130/g49139.1

Hofmann, A., Jodder, J., Xie, H., Bolhar, R., Whitehouse, M., and Elburg, M. (2022). The Archaean geological history of the Singhbhum Craton, India–a proposal for a consistent framework of craton evolution. *Earth-Science Rev* 228, 103994. doi:10.1016/j.earscirev.2022.103994

Hole, M. J. (2015). The generation of continental flood basalts by decompression melting of internally heated mantle. *Geology* 43, 311–314. doi:10.1130/g36442.1

Huppert, H. E., Stephen, R., and Sparks, J. (1985). Cooling and contamination of mafic and ultramafic magmas during ascent through continental crust. *Earth Planet. Sci. Lett* 74, 371–386. doi:10.1016/s0012-821x(85)80009-1

Irvine, T. N., and Baragar, W. R. A. (1971). A guide to the chemical classification of the common volcanic rocks. *Can. J. earth Sci* 8, 523–548. doi:10.1139/e71-055

Kamenetsky, V. S., Maas, R., Kamenetsky, M. B., Yaxley, G. M., Ehrig, K., and Zellmer, G. F., (2017). Multiple mantle sources of continental magmatism: Insights from "high-Ti" picrites of Karoo and other large igneous provinces. *Chem. Geol* 455, 22–31. doi:10.1016/j.chemgeo.2016.08.034

Korenaga, J. (2004). Mantle mixing and continental breakup magmatism. *Earth Planet. Sci. Lett* 218, 463–473. doi:10.1016/s0012-821x(03)00674-5

Krishna, A. K., Khanna, T. C., and Mohan, K. R. (2016). Rapid quantitative determination of major and trace elements in silicate rocks and soils employing fused glass discs using wavelength dispersive X-ray fluorescence spectrometry. *Spectrochim. Acta Part B At. Spectrosc* 122, 165–171. doi:10.1016/j.sab.2016.07.004

Kumar, A., Parashuramulu, V., Shankar, R., and Besse, J. (2017). Evidence for a neoarchean LIP in the Singhbhum craton, eastern India: Implications to vaalbara supercontinent. *Precambrian Res* 292, 163–174. doi:10.1016/j.precamres.2017.01.018

Le Bas, M., Maitre, R. L., Streckeisen, A., Zanettin, B., and Rocks, I. S. (1986). On the S. of IA chemical classification of volcanic rocks based on the total alkali-silica diagram. *J. petrology* 27, 745–750. doi:10.1093/petrology/27.3.745

Mandal, P. (2017). Lithospheric thinning in the eastern Indian craton: Evidence for lithospheric delamination below the archean Singhbhum craton? *Tectonophysics* 698, 91–108. doi:10.1016/j.tecto.2017.01.009

Manikyamba, C., Ray, J., Ganguly, S., Singh, M. R., Santosh, M., and Saha, A., (2015). Boninitic metavolcanic rocks and island arc tholeiites from the Older Metamorphic Group (OMG) of Singhbhum Craton, eastern India: Geochemical evidence for Archean subduction processes. *Precambrian Res* 271, 138–159. doi:10.1016/j.precamres.2015.09.028

Manu Prasanth, M., Shellnutt, J. G., and Lee, T.-Y. (2022). Secular variability of the thermal regimes of continental flood basalts in large igneous provinces since the Late Paleozoic: Implications for the supercontinent cycle. *Earth-Science Rev* 226, 103928. doi:10.1016/j.earscirev.2022.103928

Marzoli, A., Callegaro, S., Dal Corso, J., Davies, J. H., Chiaradia, M., and Youbi, N., (2018). The central atlantic magmatic province (CAMP): A review. *The Late Triassic World*, 46, 91–125.

McDonough, W. F., and Sun, S.-S. (1995). The composition of the Earth. *Chem. Geol* 120, 223–253. doi:10.1016/0009-2541(94)00140-4

Mondal, S. K., Ripley, E. M., Li, C., and Frei, R. (2006). The Genesis of archaean chromitites from the nuasahi and sukinda massifs in the Singhbhum craton, India. *Precambrian Res* 148, 45–66. doi:10.1016/j.precamres.2006.04.001

Nesbitt, R. W., Sun, S.-S., and Purvis, A. C. (1979). Komatiites; geochemistry and Genesis. *Can. Mineralogist* 17, 165–186.

Olierook, H. K., Clark, C., Reddy, S. M., Mazumder, R., Jourdan, F., and Evans, N. J. (2019). Evolution of the Singhbhum Craton and supracrustal provinces from age, isotopic and chemical constraints. *Earth-Science Rev* 193, 237–259. doi:10.1016/j.earscirev.2019.04.020

Pandey, O. P., Mezger, K., Ranjan, S., Upadhyay, D., Villa, I. M., and Nägler, T. F., (2019). Genesis of the Singhbhum craton, eastern India; implications for archean crust-mantle evolution of the earth. *Chem. Geol* 512, 85–106. doi:10.1016/j.chemgeo.2019.02.040

Pandey, O. P., Mezger, K., Upadhyay, D., Paul, D., Singh, A. K., and Söderlund, U., (2021). Major-trace element and Sr-Nd isotope compositions of mafic dykes of the Singhbhum Craton: Insights into evolution of the lithospheric mantle. *Lithos* 382, 105959. doi:10.1016/j.lithos.2020.105959

Pearce, J. A. (2008). Geochemical fingerprinting of oceanic basalts with applications to ophiolite classification and the search for Archean oceanic crust. *Lithos* 100, 14–48. doi:10.1016/j.lithos.2007.06.016

Pertermann, M., and Hirschmann, M. M. (2003). Partial melting experiments on a MORB-like pyroxenite between 2 and 3 GPa: Constraints on the presence of pyroxenite in basalt source regions from solidus location and melting rate. *J. Geophys. Res. Solid Earth* 108. doi:10.1029/2000jb000118

Putirka, K. D. (2008). Thermometers and barometers for volcanic systems. *Rev. mineralogy Geochem* 69, 61–120. doi:10.2138/rmg.2008.69.3

Ravindran, A., Mezger, K., Balakrishnan, S., and Berndt, J. (2021). Hf-Nd isotopes from ultramafic and mafic rocks in the Western Dharwar Craton, India, record early Archean mantle heterogeneity. *Lithos* 404, 106491. doi:10.1016/j.lithos.2021.106491

Roy, A., Sarkar, A., Jeyakumar, S., Aggrawal, S. K., Ebihara, M., and Satoh, H. (2004). Late archaean mantle metasomatism below eastern Indian craton: Evidence from trace elements, REE geochemistry and Sr—Nd—O isotope systematics of ultramafic dykes. *J. Earth Syst. Sci* 113, 649–665. doi:10.1007/bf02704027

Rudnick, R. L., and Gao, S. (2014). "Composition of the continental crust," in *Treatise on Geochemistry*. Editors H. D. Holland and K. K. Turekian. second edition Elsevier. Netherlands, UK. doi:10.1016/B978-0-08-095975-7.00301-6

Satyanarayanan, M., Balaram, V., Sawant, S. S., Subramanyam, K. S. V., Krishna, G. V., and Dasaram, B., (2018). Rapid determination of REEs, PGEs, and other trace elements in geological and environmental materials by high resolution inductively coupled plasma mass spectrometry. *At. Spectrosc* 39, 1–15. doi:10.46770/as.2018.01.001

Shankar, R., Sarma, D. S., Babu, N. R., and Parashuramulu, V. (2018). Paleomagnetic study of 1765 Ma dyke swarm from the Singhbhum craton: Implications to the paleogeography of India. *J. Asian Earth Sci* 157, 235–244. doi:10.1016/j.jseaes.2017.08.026

Shellnutt, J. G., Ur Rehman, H., and Manu Prasanth, M. P. (2021). Insight into crustal contamination and hydrothermal alteration of the Panjal Traps (Kashmir) from O-isotopes. *Int. Geol. Rev* 64, 1556–1573. doi:10.1080/00206814.2021.1941324

Söderlund, U., Hofmann, A., Klausen, M. B., Olsson, J. R., Ernst, R. E., and Persson, P.-O. (2010). Towards a complete magmatic barcode for the Zimbabwe craton: Baddeleyite U–Pb dating of regional dolerite dyke swarms and sill complexes. *Precambrian Res* 183, 388–398. doi:10.1016/j.precamres.2009.11.001

Sreenivas, B., Dey, S., Rao, Y. B., Kumar, T. V., Babu, E., and Williams, I. S. (2019). A new cache of Eoarchaean detrital zircons from the Singhbhum craton, eastern India and constraints on early Earth geodynamics. *Geosci. Front* 10, 1359–1370. doi:10.1016/j.gsf.2019.02.001

Srivastava, R. K., Söderlund, U., Ernst, R. E., Mondal, S. K., and Samal, A. K. (2019). Precambrian mafic dyke swarms in the Singhbhum craton (eastern India) and their links with dyke swarms of the eastern Dharwar craton southern India. *Precambrian Res* 329, 5–17. doi:10.1016/j.precamres.2018.08.001

Stracke, A., Scherer, E. E., and Reynolds, B. C. (2014). "Application of isotope dilution in geochemistry," in *Treatise on Geochemistry*. Editors H. D. Holland and K. K. Turekian. Second Edition Netherlands, UK: Elsevier, 71–86. doi:10.1016/B978-0-08-095975-7.01404-2

Su, B., Zhang, H., Asamoah, S. P., Qin, K., Tang, Y., and Ying, J., (2010). Garnet-spinel transition in the upper mantle: Review and interpretation. *J. Earth Sci* 21, 635–640. doi:10.1007/s12583-010-0117-x

Sun, S.-S., and McDonough, W. F. (1989). Chemical and isotopic systematics of oceanic basalts: Implications for mantle composition and processes. *Geol. Soc. Lond. Spec. Publ* 42, 313–345. doi:10.1144/gsl.sp.1989.042.01.19

Tang, Y.-J., Zhang, H.-F., Ying, J.-F., and Su, B.-X. (2013). Widespread refertilization of cratonic and circum-cratonic lithospheric mantle. *Earth-Science Rev* 118, 45–68. doi:10.1016/j.earscirev.2013.01.004

Tegner, C., Michelis, S. A., McDonald, I., Brown, E. L., Youbi, N., and Callegaro, S., (2019). Mantle dynamics of the central atlantic magmatic province (CAMP): Constraints from platinum group, gold and lithophile elements in flood basalts of Morocco. *J. Petrology* 60, 1621–1652. doi:10.1093/petrology/egz041

Upadhyay, D., Chattopadhyay, S., Kooijman, E., Mezger, K., and Berndt, J. (2014). Magmatic and metamorphic history of Paleoarchean tonalite–trondhjemite–granodiorite (TTG) suite from the Singhbhum craton, eastern India. *Precambrian Res* 252, 180–190. doi:10.1016/j.precamres.2014.07.011

Upadhyay, D., Chattopadhyay, S., and Mezger, K. (2019). Formation of paleoarchean-mesoarchean Na-rich (TTG) and K-rich granitoid crust of the Singhbhum craton, eastern India: Constraints from major and trace element geochemistry and Sr-Nd-Hf isotope composition. *Precambrian Res* 327, 255–272. doi:10.1016/j.precamres.2019.04.009

Vance, D., and Thirlwall, M. (2002). An assessment of mass discrimination in MC-ICPMS using Nd isotopes. *Chem. Geol* 185, 227–240. doi:10.1016/s0009-2541(01)00402-8

Wang, W., Spencer, C., Pandit, M. K., Wu, Y.-B., Zhao, J.-H., and Zheng, J.-P., (2022). Crustal evolution and tectonomagmatic history of the Indian Shield at the periphery of supercontinents. *Geochimica Cosmochimica Acta* 341, 90–104. doi:10.1016/j.gca.2022.10.040

Whalen, L., Gazel, E., Vidito, C., Puffer, J., Bizimis, M., and Henika, W., (2015). Supercontinental inheritance and its influence on supercontinental breakup: The C entral A tlantic M agmatic P rovince and the breakup of P angea. *Geochem. Geophys. Geosystems* 16, 3532–3554. doi:10.1002/2015gc005885

Wilson, J. F. (1990). A craton and its cracks: Some of the behaviour of the Zimbabwe block from the late archaean to the mesozoic in response to horizontal movements, and the significance of some of its mafic dyke fracture patterns. *J. Afr. Earth Sci. (and the Middle East)* 10, 483–501. doi:10.1016/0899-5362(90)90101-j

Wilson, M. (1989). *Igneous petrogenesis*. Dordrecht, Netherlands: Springer.

Winchester, J. A., and Floyd, P. A. (1976). Geochemical magma type discrimination: Application to altered and metamorphosed basic igneous rocks. *Earth and Planetary Science Letters* 28, 459–469. doi:10.1016/0012-821x(76)90207-7

Workman, R. K., and Hart, S. R. (2005). Major and trace element composition of the depleted MORB mantle (DMM). *Earth and Planetary Science Letters* 231, 53–72. doi:10.1016/j.epsl.2004.12.005

Zheng, Y.-F. (2019). Subduction zone geochemistry. *Geoscience Frontiers* 10, 1223–1254. doi:10.1016/j.gsf.2019.02.003

Zhu, R., Zhao, G., Xiao, W., Chen, L., and Tang, Y. (2021). Origin, accretion, and reworking of continents. *Reviews of Geophysics* 59, doi:10.1029/2019rg000689